Contrasting evolution of sea surface temperature in the Benguela upwelling system under natural and anthropogenic climate forcings

Guillaume Leduc,[1] Caren T. Herbert,[2] Thomas Blanz,[1] Philippe Martinez,[3] and Ralph Schneider[1]

Received 15 June 2010; revised 20 August 2010; accepted 26 August 2010; published 27 October 2010.

[1] We present alkenone-derived Sea Surface Temperature (SST) records from three marine cores collected within the southern Benguela Upwelling System (BUS) spanning the last 3 ka. The SST evolution over the last 3 millennia is marked by aperiodic millennial-scale oscillations that broadly correspond to climatic anomalies identified over the North Atlantic region. The BUS SST data further suggest cooling and warming trends opposite to the temperature evolution in the Moroccan upwelling region and in Antarctica. In contrast, the last decades are marked by a cooling of unprecedented magnitude in both the Benguela and Moroccan upwelling systems, which is not observed in the Antarctic record. These contrasted responses in Atlantic upwelling systems triggered by natural and anthropogenic forcings shed light on how different climatic mechanisms are mediated by ocean-atmosphere interactions and transmitted to the geological records of past and present climate changes. **Citation:** Leduc, G., C. T. Herbert, T. Blanz, P. Martinez, and R. Schneider (2010), Contrasting evolution of sea surface temperature in the Benguela upwelling system under natural and anthropogenic climate forcings, *Geophys. Res. Lett.*, *37*, L20705, doi:10.1029/2010GL044353.

1. Introduction

[2] Global compilations of proxy records covering the last millennium indicate that multi-century climate variations such as the Medieval Climate Anomaly (MCA) and the Little Ice Age (LIA) were not uniformly distributed [*Jones et al.*, 2009; *Mann et al.*, 2009; *Trouet et al.*, 2009]. Instrumental data rather indicate that the warming recorded over the last decades is global [see, e.g., *Hansen et al.*, 2006]. However, as continents warm faster than oceans under anthropogenic global warming [*Meehl et al.*, 2007], increased land-sea pressure gradients and local wind stress can locally trigger coastal upwelling intensification and thus cause local surface ocean cooling in a warming world [*Bakun*, 1990]. Accordingly, an alkenone-derived record of Sea Surface Temperature (SST) from the Northwestern African margin provided evidence for recent coastal upwelling intensification [*McGregor et al.*, 2007]. In that record, an accelerated cooling trend was observed over the last decades along the Moroccan coast caused by a recent increase in coastal upwelling, likely linked to strengthened winds blowing alongshore and increasing Ekman pumping [*McGregor et al.*, 2007]. Further investigations of recent upwelling variability outside of the northern tropical Atlantic are needed to address whether the recent Moroccan upwelling increase is a common feature of eastern boundary upwelling systems or if it is related to a local response confined to the northeastern Atlantic exclusively.

[3] Here we present new alkenone-derived SST records from three shallow marine cores collected from the Holocene mudbelt deposited on the South African shelf under the southern Benguela Upwelling System (BUS) (Figure 1). Two of them are short cores that preserved the water-sediment interface and provide SST changes over the last decades only. These are complemented by a Late Holocene (LH) SST record stemming from a third gravity core that enable us to compare the SST evolution over the last three millennia with the recent SST trend, considered as a response to anthropogenic climate forcing that occurred over the last decades.

2. Regional Settings

[4] The BUS is one of the four Eastern Boundary Upwelling Ecosystems, and among the most productive regions of the World Ocean. Regional upwelling cells are located along the southern Namibian and northern South African coasts, and are dynamically related to trade wind-induced Ekman transport perpendicular to the coastline (Figure 1).

[5] The Orange River Holocene mudbelt is a shelf-transgressive deposit that geographically corresponds to the spatial extent of the southern BUS (Figures 1a and 1b), and is related to fluvial sediment transport induced by landmass erosion within the Southwestern African continental river catchments [*Herbert and Compton*, 2007]. This mudbelt provides Holocene sedimentary records with a very high time resolution [*Herbert and Compton*, 2007].

[6] The seasonal cycles of SST, productivity and total vertical water mass transport are relatively weak as compared to other upwelling systems [*Chavez and Messié*, 2009]. High productivity is sustained year-round through intraseasonal eddy-induced changes in upwelling [*Chavez and Messié*, 2009]. Recent hydrographic evolution of the southern BUS indicates that a striking relationship exists between regional temperature and chlorophyll concentra-

[1]Institute of Earth Sciences, Kiel University, Kiel, Germany.
[2]Department of Geological Sciences, University of Cape Town, Rondebosch, South Africa.
[3]Université Bordeaux 1, UMR CNRS 5805 EPOC, Talence, France.

0094-8276/10/2010GL044353

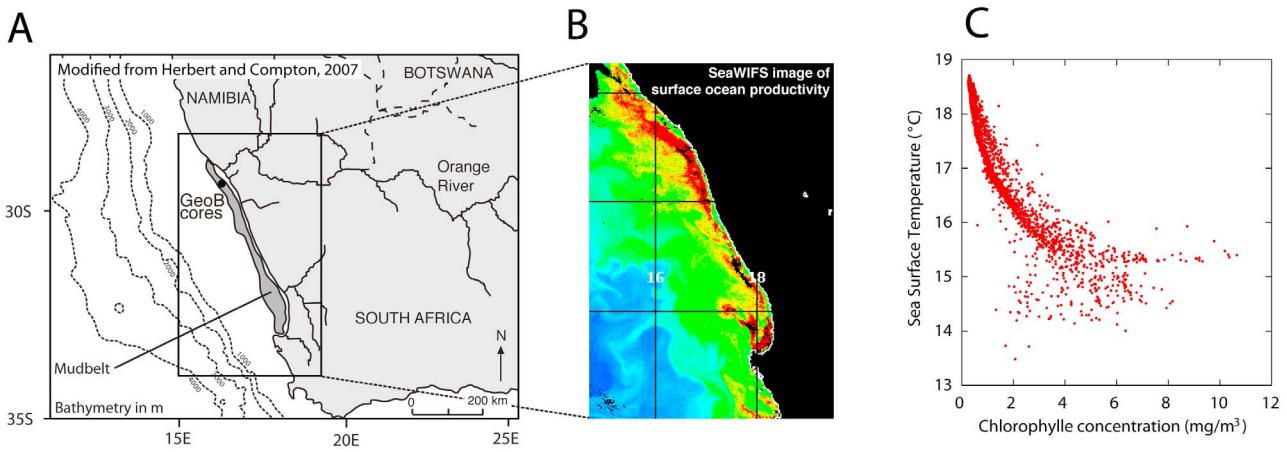

Figure 1. (a) Map of southwestern Africa indicating GeoB cores locations. The mudblet where Holocene sedimentary sequences with high accumulation rates were deposited is highlighted in grey. (b) Ocean color of the southern BUS derived from SeaWIFS imaging (http://seawifs.gsfc.nasa.gov/). Increasing chlorophyll concentrations are depicted from blue to red color on a rainbow color scale. (c) Scatterplot of temperature and *chlorophyll a* concentrations averaged over the 2002–2007 period and corresponding to the oceanic region highlighted in Figure 1b. The plot was generated using the Giovanni (Ocean Color Radiometry Online Visualization and Analysis) tool available at http://daac.gsfc.nasa.gov/giovanni/.

tions (Figure 1c), suggesting that both productivity and SST are appropriate parameters to track the BUS evolution.

3. Material and Methods

[7] Marine sediment gravity core GeoB8331-4 (29°08′07.2″S, 16°42′59.4″E, 97 m depth), and multicores GeoB8331-2 (same station as GeoB8331-4) and GeoB8332-3 (29°07′39.6″S, 16°39′33.6″E, 115 m depth) were collected in 2003 close to the Orange River mouth (Figure 1a).

[8] The di- and triunsaturated C_{37} methyl alkenone $C_{37:2}$ and $C_{37:3}$ were extracted and quantified at Kiel University following the analytical procedure described in *Rincón-Martínez et al.* [2010]. The alkenone unsaturation index $U^{k'}_{37}$ was calculated using the ratio $(C_{37:2})/(C_{37:2} + C_{37:3})$. To translate the $U^{k'}_{37}$ index into SST we used the global core-top calibration of *Müller et al.* [1998].

[9] The age model of core GeoB8331-4 is extensively described by *Herbert and Compton* [2007], and is derived from seven radiocarbon dates measured on the gastropod species *Nassarius vinctus* using the *Fairbanks et al.* [2005] calibration program and a constant reservoir age of 550 years. Grain size analyses performed downcore [*Herbert and Compton*, 2007] were used as a diagnostic for winnowed sediments (Figure 2a). Winnowed sedimentary horizons indicated by sharp increases in the coarse silt size fraction only occur below ~500 cm core depth. They broadly correspond to intervals of decreased sedimentation rates and may compromise the integrity of alkenone-derived SST record for ages older than ~3000 years BP [*Mollenhauer et al.*, 2003] (Figure 2a). The coarse-silt size fraction of the upper 5 m remained below

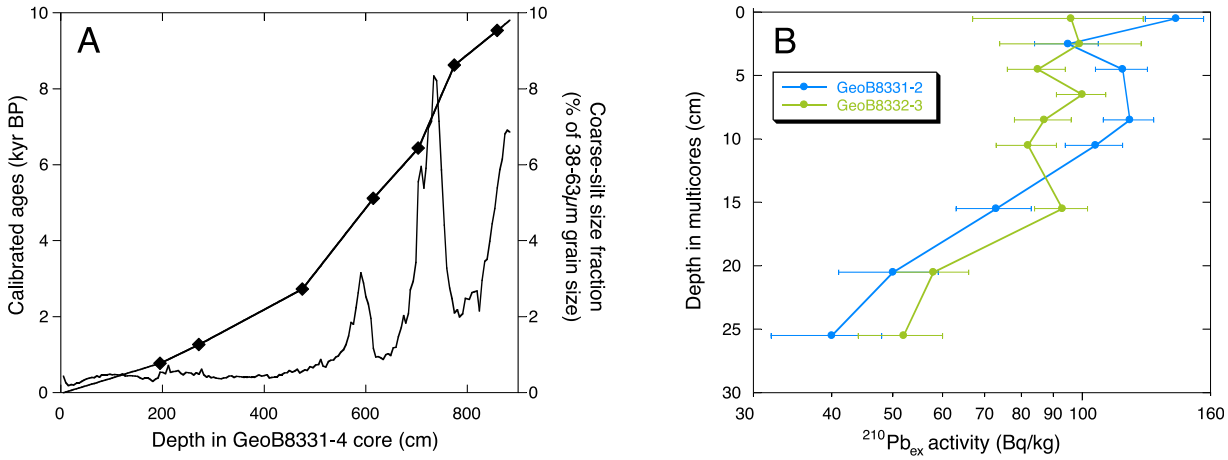

Figure 2. (a) Radiocarbon-based age model of GeoB8331-4 gravity core and coarse-silt size fraction as published in the work of *Herbert and Compton* [2007]. The black lines connecting the filled diamonds represent the depth-age relationship. The black curve indicates the coarse-silt size fraction measurements performed downcore [*Herbert and Compton*, 2007]. (b) Measurements of $^{210}Pb_{ex}$ sedimentary activity of multicores GeoB8331-2 (blue curve) and GeoB8332-3 (green curve).

1%, suggesting a continuous local mudbelt deposition with sedimentation rates higher than 1 mm/year over the last 3 ka.

[10] $^{210}Pb_{ex}$ measurements were performed on multicores GeoB8331-2 and GeoB8332-3 using gamma spectrometry (Figure 2b). Both multicores indicate a biological mixing zone of ~10 to 15 cm thick (Figure 2b). Multicore GeoB8331-2 apparently bears 4 to 5 $^{210}Pb_{ex}$ measurements performed on sedimentary horizons from below the biological mixed layer (Figure 2b). We hence derived linear sedimentation rates for this core assuming a constant initial $^{210}Pb_{ex}$ concentration and a constant sedimentation rate. The calculated linear sedimentation rates for core GeoB8331-2 are 4.7 and 4.8 mm/yr when the biological mixing zone thickness was set up at 8.5 and 10.5 cm, respectively. Assuming an unchanged sedimentation rate for the bioturbated zone, $^{210}Pb_{ex}$ measurements suggest a bottom age slightly older than 60 years as compared to the multicore core-top age, indicating that multicores may cover the 1940–2000 A.D. time period. As $^{210}Pb_{ex}$ was detected in GeoB8331-4 gravity core (84 and 43 Bq/kg at 3 and 8 cm depth, respectively; not shown), its core-top age was set up at 0 kyr BP (i.e. 1950 A.D., Figure 2a). The GeoB8331-2 multicore sedimentation rate is about two times higher than the linear sedimentation rate of the upper part of the gravity core GeoB8331-4 as estimated from the last radiocarbon dating and the core top, which is expected because the sediment compaction should be reduced in the multicore. The gravity core and multicores SST records provide ~30 and ~2 years resolution, respectively.

4. Results and Discussion

[11] In an attempt to improve the understanding of alkenone-based SST reconstructions in terms of seasonality as hypothesized in *Leduc et al.* [2010], *Schneider et al.* [2010] have used satellite data for mapping the existing relationship between the annual cycles of SST and of primary productivity. The seasonality index developed by *Schneider et al.* [2010] broadly predicts an increased primary productivity when SST are below the mean-annual value at mid-latitudes, because upwelling bringing nutrients to the sea surface synchronously act to trigger algal blooming and to decrease SST (Figure 1c). We hence interpret the alkenone-derived SST records of the BUS as representative of the SST during upwelling events.

[12] The BUS SST history as estimated from the GeoB8331-4 gravity core for the last 3 ka reveals a series of aperiodic SST changes of ~1°C in amplitude at the multi-centennial to millennial timescale (Figure 3c). Two SST maxima peaked at ~700 and 2000 years BP. Given the limits of radiocarbon dating by using constant marine reservoir ages, these BUS SST maxima correlate with warm periods in Greenland, but with cold periods in the SST record from the Moroccan upwelling system as well as in air temperature record above East Antarctica (Figures 3a–3d). Conversely, the BUS SST minimum culminating at ~1300 years BP and corresponding to cold temperatures over Greenland is coeval with warmer periods in the Moroccan upwelling system and over Antarctica (Figures 3a–3d). A similar opposite temperature behaviour between the BUS and the Morrocan upwelling as well as East Antarctica seems likely for the BUS cold period at about ~2500 years BP, but the shortness of the Moroccan record prevents a robust evidence for such an opposite SST evolution back to 3000 years BP. Similarly, the temperature times series lack a clear antiphase behaviour over the last 500 years BP. Instead, the marine temperature records suggest a joint cooling mainly after 200 years BP, while the Greenland and Antarctic temperatures underwent no significant change at the centennial scale. Interestingly, this joint cooling trend in the marine temperature records from both upwelling regions is reinforced over the last ~50 to 30 years (Figures 3e–3f).

[13] Both multicores from BUS provided SST records marked by a cooling of ~2°C over the last 30 years (Figure 3f), synchronous with an increase in alkenone concentration (Figure 3g). The latter confirms a coccolithophorid productivity increase related to a recent increase in coastal upwelling (Figure 1c). We are confident in the significance of the SST drop recorded over the last 30 years because the cooling trend is clearly documented by about 10 data points in both multicores that were collected 6 km apart from each other. Additionally, the magnitude of the most recent SST decline is four times larger than the expected SST decline due to long-term oxic degradation in an extreme case scenario, suggesting that any preservation effect is unlikely to have artificially produced the SST trend in the uppermost multicore sections [*Huguet et al.*, 2009].

[14] In the bipolar seesaw conceptual model, the North and South Atlantic climatic signals are expected to be in antiphase [*Stocker and Johnsen*, 2003]. As continents have less thermal inertia than oceans, the land-ocean atmospheric pressure gradients are expected to accommodate to any regional climate shift by modulating the intensity of the winds blowing along the coastline, so that the associated intensity of the eastern boundary upwelling systems would adjust accordingly to climate change. In such a scenario, regional climate warming or cooling in any hemisphere would tend to favor coastal upwelling intensity to increase or decrease, respectively [*Bakun*, 1990]. If one further assumes that ice core temperature records provide information adequate to monitor hemispheric-scale temperature background at mid- to high-latitudes [*Jones and Mann*, 2004], then the response of upwelling intensity can be tested by comparing the temperature records from Atlantic upwelling areas with those from Greenland and Antarctic ice cores.

[15] The SST data we report here suggest that such an interhemispheric antiphase teleconnection existed at millennial and multi-centennial timescales, and that eastern Atlantic upwelling systems respond to this seesaw by showing stronger upwelling-induced coolings during warm periods within a given hemisphere as indicated in the ice core temperature records (Figures 3a–3d). As a consequence of the bipolar climate seesaw, the maxima in BUS SST should correspond to SST minima off Morocco and vice-versa. For the last millennia this synchronicity is apparent from both the BUS and Moroccan SST polynomial fit curves (Figures 3b–3c). This confirms the hypothesis by *Bakun* [1990] that local upwelling responds to hemisphere-scale climate features even for those inherent to millennial and multi-centennial climate variability, although this hypothesis was raised with respect to the global climate warming occurring nowadays. Since the 19th century, the interhemispheric antiphase behavior is likely to be superimposed to another forcing mechanism, resulting in continuous cooling in both upwelling regions. Whether the latter result relates to global climate warming or to another unidentified feedback that has oper-

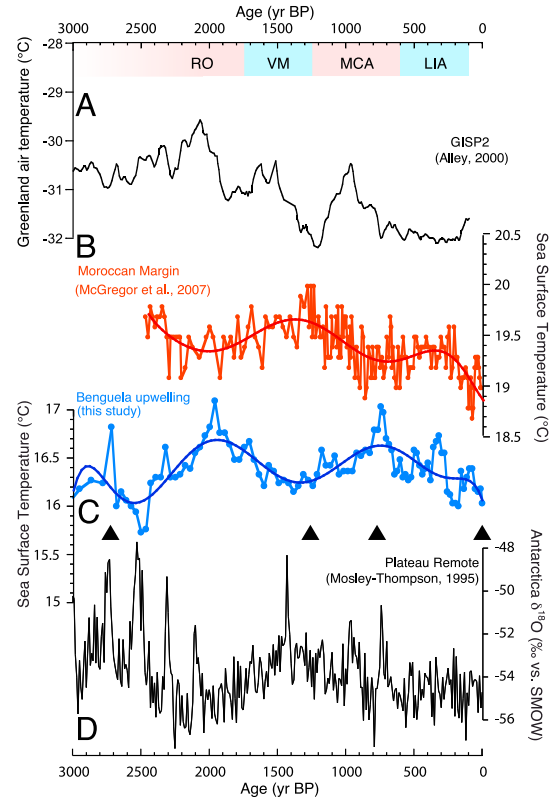

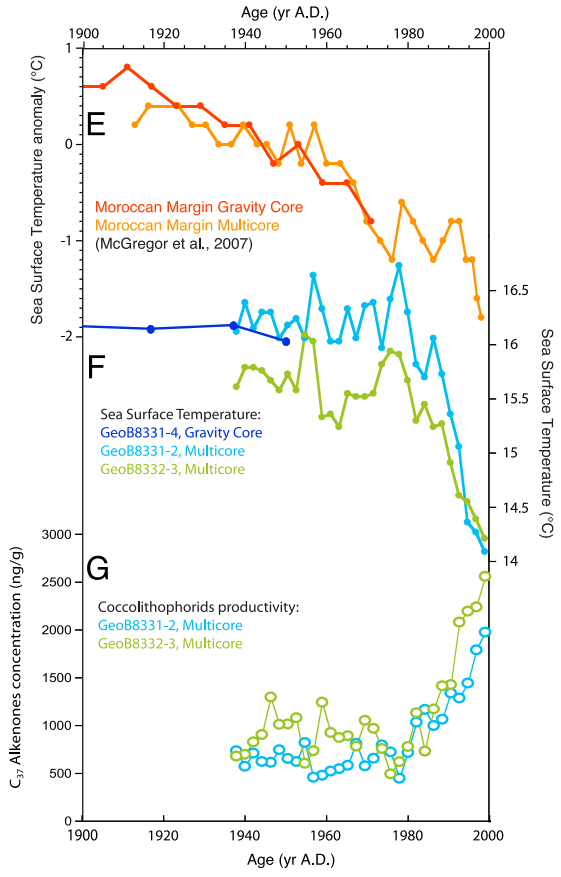

ated over the last 200 years cannot be assessed from the sedimentary archives at hand.

[16] The mode of coastal upwelling response to anthropogenic global warming was recently investigated for the 1960–2000 A.D. time period using various upwelling indicators in the four major eastern boundary coastal upwelling systems [*Narayan et al.*, 2010]. In their study, *Narayan et al.* [2010] have used wind speed and SST data to evidence a recent wind-induced upwelling acceleration that was particularly marked within the southern BUS region, and to a lesser extent in the three other eastern boundary upwelling systems. The new paleotemperature records seem to validate the observations based on instrumental data by showing substantial cooling along the Moroccan Margin [*McGregor et al.*, 2007], in the BUS (this study) and probably along the Peruvian Margin as well [*Bouloubassi et al.*, 2009; *Gutiérrez et al.*, 2009; *Sifeddine et al.*, 2008].

[17] Upwelling-driven productivity changes may also have important implications for subsurface oxygenation in tropical Oxygen Minimum Zones (OMZs). A trend toward oxygen depletion was recorded over the last decades in all the present-day tropical OMZs [*Stramma et al.*, 2008]. Although increased stratification globally affects oxygen solubility and oceanic ventilation that may trigger tropical OMZs deoxygenation, an increase in biologically-mediated oxygen consumption may regionally contribute to oxygen depletion if tropical coastal upwelling systems would tend to increase as well.

5. Conclusions

[18] We have investigated the influence of natural BUS variability over the last 3 millennia and the recent BUS response to anthropogenic climate forcing as revealed by the alkenone-derived SST records estimated from marine sediment cores. Our results suggest a close relationship between the BUS SST changes at the multi-centennial timescale over the last millennia with interhemisperic climate antiphase behavior and probably with global climate change at the historical time scale. When the BUS SST record is compared to the ones from the Moroccan upwelling system and to Greenland and Antarctica temperature records, it appears that (i) both upwelling systems have virtually evolved in

Figure 3. (a) Greenland air temperature recorded at GISP2 site [*Alley*, 2000]. (b) Moroccan Margin SST changes (red curve [*McGregor et al.*, 2007]). (c) Benguela upwelling SST changes estimated from GeoB8331-4 gravity core (blue curve, this study). (d) Antarctica air temperature derived from oxygen stable isotopes at Plateau Remote site [*Mosley-Thompson*, 1995]. (e) SST from Moroccan Margin spanning the 20th century [*McGregor et al.*, 2007]. (f) Benguela upwelling SST records spanning the 20th century (this study). (g) Benguela upwelling productivity spanning the 20th century as estimated by C_{37} Alkenone concentration (this study). Historical climatic anomalies initially identified in Europe are reported at the top (RO = Roman Optimum, VM = Vandal Minimum, MCA = Medieval Climate Anomaly, LIA = Little Ice Age). Nonic polynomial fits are reported for SST records depicted in Figures 3b and 3c; note that the roots of polynomial fits of the BUS and Moroccan upwelling systems are synchronous.

antiphase, and that (ii) each upwelling system has virtually evolved in antiphase with the high-latitude air temperature record from its own hemisphere. This observation can be explained by invoking an interhemispheric bipolar seesaw together with local land-sea interactions where coastal upwelling tends to increase whenever the regional climate warms.

[19] On the other hand, both upwelling systems seem to have been drastically affected by an increase in coastal upwelling presumably linked to anthropogenic global warming through local land-ocean interactions. This latter result suggests that the eastern boundary upwelling systems are very sensitive to anthropogenic global warming, one observation that has further implications on the future evolution of biogeochemical cycles since it provides a mechanism that contributes to the recent expanse of tropical OMZs.

[20] These contrasting modes of interhemispheric upwelling evolution in the tropical Atlantic Ocean that are probably triggered by different forcings illustrate the need for mapping efforts of proxy-derived past climate trends over a hierarchy of timescales to identify the impact of natural and anthropogenic climate forcings on regional climate evolution.

[21] **Acknowledgments.** We thank two anonymous reviewers for thorough comments. We thank Valérie Masson-Delmotte for providing the Plateau Remote ice core data. Assistance with alkenone analysis by S. Koch is greatly acknowledged. This work was financed by the German Research Foundation (DFG) in the framework of the German Research Priority Program SPP1266 (INTERDYNAMIK) and for RV *METEOR* cruise M57-1 to the southwest African margin executed by the DFG Research Centre Ocean Margins at Bremen University.

References

Alley, R. B. (2000), The Younger Dryas cold interval as viewed from central Greenland, *Quat. Sci. Rev.*, *19*, 213–226, doi:10.1016/S0277-3791(99)00062-1.

Bakun, A. (1990), Global climate change and intensification of coastal ocean upwelling, *Science*, *247*, 198–201, doi:10.1126/science.247.4939.198.

Bouloubassi, I., et al. (2009), Cooling trend and enhancement of productivity in the upwelling off Peru since the late 19th century, *Eos Trans. AGU*, *90*(52), Fall Meet. Suppl., Abstract PP41B-1520.

Chavez, F. P., and M. Messié (2009), A comparison of eastern boundary upwelling ecosystems, *Prog. Oceanogr.*, *54*, 251–264.

Fairbanks, R. G., et al. (2005), Radiocarbon calibration curve spanning 0 to 50,000 years BP based on paired $^{230}Th/^{234}U/^{238}U$ and ^{14}C dates on pristine corals, *Quat. Sci. Rev.*, *24*, 1781–1796, doi:10.1016/j.quascirev.2005.04.007.

Gutiérrez, D., et al. (2009), Rapid reorganization in ocean biogeochemistry off Peru towards the end of the Little Ice Age, *Biogeosciences*, *6*, 835–848, doi:10.5194/bg-6-835-2009.

Hansen, J., M. Sato, R. Ruedy, K. Lo, D. W. Lea, and M. Medina-Elizade (2006), Global temperature change, *Proc. Natl. Acad. Sci. U. S. A.*, *103*, 14,288–14,293, doi:10.1073/pnas.0606291103.

Herbert, C. T., and J. S. Compton (2007), Geochronology of Holocene sediments on the western margin of South Africa, *S. Afr. J. Geol.*, *110*, 327–338, doi:10.2113/gssajg.110.2-3.327.

Huguet, C., J.-H. Kim, G. J. de Lange, J. S. Sinninghe Damsté, and S. Schouten (2009), Effects of long-term oxic degradation on the $U^{k'}_{37}$, TEX_{86} and BIT organic proxies, *Org. Geochem.*, *40*, 1188–1194, doi:10.1016/j.orggeochem.2009.09.003.

Jones, P. D., and M. E. Mann (2004), Climate over past millennia, *Rev. Geophys.*, *42*, RG2002, doi:10.1029/2003RG000143.

Jones, P. D., et al. (2009), High-resolution paleoclimatology of the last millennium: A review of recent status and future prospects, *Holocene*, *19*, 3–49, doi:10.1177/0959683608098952.

Leduc, G., R. R. Schneider, J.-H. Kim, and G. Lohmann (2010), Holocene and Eemian sea surface temperature trends as revealed by alkenone and Mg/Ca paleothermometry, *Quater. Sci. Rev.*, *29*, 989–1004, doi:10.1016/j.quascirev.2010.01.004.

Mann, M. E., et al. (2009), Global signatures and dynamical origins of the Little Ice Age and Medieval Climate Anomaly, *Science*, *326*, 1256–1260, doi:10.1126/science.1177303.

McGregor, H. V., M. Dima, H. W. Fischer, and S. Mulitza (2007), Rapid 20th-century increase in coastal upwelling off northwest Africa, *Science*, *315*, 637–639, doi:10.1126/science.1134839.

Meehl, G. A., et al. (2007), Global climate projections, in *Climate Change 2007: The Physical Science Basis: Contribution of Working Group I to the Fourth Assessment Report of the Intergovernmental Panel on Climate Change*, edited by S. Solomon et al., pp. XX–XX, Cambridge Univ. Press, New York.

Mollenhauer, G., T. I. Eglington, N. Ohkouchi, R. R. Schneider, P. J. Müller, P. M. Grootes, and J. Rullkötter (2003), Asynchronous alkenone and foraminifera records from the Benguela upwelling system, *Geochim. Cosmochim. Acta*, *67*, 2157–2171, doi:10.1016/S0016-7037(03)00168-6.

Mosley-Thompson, E. (1995), Holocene climate changes recorded in an East Antarctica ice core, in *Climatic Variations and Forcing Mechanisms of the Last 2,000 Years*, vol. 41, edited by P. Jones, R. Bradley, and J. Jouzel, pp. 263–279, NATO Adv. Res., Berlin.

Müller, P. J., G. Kirst, G. Ruhland, I. von Storch, and A. Rosell-Melé (1998), Calibration of alkenone paleotemerature index $U^{k'}_{37}$ based on core-tops from the eastern South Atlantic and the global ocean (60°N-60°S), *Geochim. Cosmochim. Acta*, *62*, 1757–1772, doi:10.1016/S0016-7037(98)00097-0.

Narayan, N., A. Paul, S. Mulitza, and M. Schulz (2010), Trends in coastal upwelling intensity during the late 20th century, *Ocean Sci. Discuss.*, *7*, 335–360, doi:10.5194/osd-7-335-2010.

Rincón-Martínez, D., et al. (2010), More humid interglacials in Ecuador during the past 500 kyr linked to latitudinal shifts of the equatorial front and the Intertropical Convergence Zone in the eastern tropical Pacific, *Paleoceanography*, *25*, PA2210, doi:10.1029/2009PA001868.

Schneider, B., G. Leduc, and W. Park (2010), Disentangling seasonal signals in Holocene climate trends by satellite-model-proxy integration, *Paleoceanography*, doi:10.1029/2009PA001893, in press.

Sifeddine, A., et al. (2008), Laminated sediments from the central Peruvian continental slope: A 500 year record of upwelling system productivity, terrestrial runoff and redox conditions, *Prog. Oceanogr.*, *79*, 190–197, doi:10.1016/j.pocean.2008.10.024.

Stocker, T. F., and S. J. Johnsen (2003), A minimum thermodynamic model for the bipolar seesaw, *Paleoceanography*, *18*(4), 1087, doi:10.1029/2003PA000920.

Stramma, L., G. C. Johnson, J. Sprintall, and V. Mohrholz (2008), Expanding oxygen-minimum zones in the tropical oceans, *Science*, *320*, 655–658, doi:10.1126/science.1153847.

Trouet, V., J. Esper, N. E. Graham, A. Baker, J. D. Scourse, and D. V. Frank (2009), Persistent positive North Atlantic Oscillation mode dominated the Medieval Climate Anomaly, *Science*, *324*, 78–80, doi:10.1126/science.1166349.

T. Blanz, G. Leduc, and R. Schneider, Institute of Earth Sciences, Kiel University, Ludewig-Meyn-Str. 10 D-24118 Kiel, Germany. (gl@gpi.uni-kiel.de)

C. T. Herbert, Department of Geological Sciences, University of Cape Town, Private Bag X3, Rondebosch 7701, South Africa.

P. Martinez, Université Bordeaux 1, UMR CNRS 5805 EPOC, Avenue des facultés, F-33405 Talence, France.